



University of  
New Haven

University of New Haven

Digital Commons @ New Haven

---

Master's Theses

Student Works

---

12-2019

## Measurement of Polishing Rate as a Function of Pad-Independent Abrasive Friction for Chemical Mechanical Polishing

Christopher McGowan

Follow this and additional works at: <https://digitalcommons.newhaven.edu/masterstheses>



Part of the [Mechanical Engineering Commons](#)

---



University of New Haven

**Measurement of Polishing Rate as a Function of Pad-Independent  
Abrasive Friction for Chemical Mechanical Polishing**

A RESEARCH PROJECT

Submitted in partial fulfillment of the requirements of

MASTER OF SCIENCE IN MECHANICAL ENGINEERING

BY

Christopher McGowan

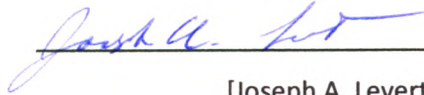
University of New Haven

West Haven, Connecticut

December 2019

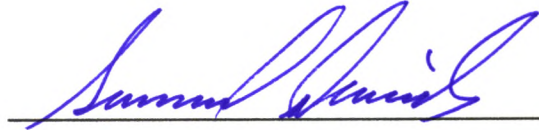
**Measurement of Polishing Rate as a Function of Pad-Independent  
Abrasive Friction for Chemical Mechanical Polishing**

APPROVED BY



[Joseph A. Levert, Ph.D.]

Thesis Adviser



[Sam B. Daniels, Ph.D.]

Committee Member



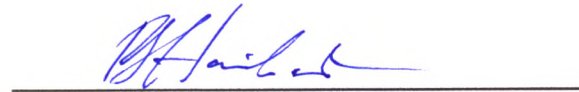
[Eric Dieckman, Ph.D.]

Committee Member



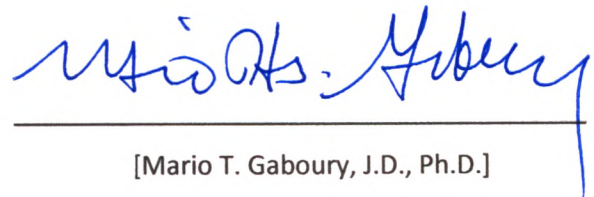
[Eric Dieckman, Ph.D.]

Program Coordinator



[Ronald S. Harichandran, Ph.D., P.E., F.ASCE

Dean of the College



[Mario T. Gaboury, J.D., Ph.D.]

Provost

## Acknowledgements

I would like to thank:

Dr. Joseph Levert, whose work this experiment is based on and whose guidance shaped the project as it grew.

Michele Berman, without whom this experiment would not have been possible given its demand of chemistry lab space.

Cailin McGowan, whose confidence saw me take on this challenge and whose support saw me through it.

And the University of New Haven for the opportunity.

## TABLE OF CONTENTS

Abstract.....	v
List of Figures.....	vi
List of Symbols Used in this Work.....	vii
Introduction.....	1
Model.....	6
Test Procedure.....	10
Results.....	14
Discussion.....	19
Conclusion.....	24
Works Cited.....	26

## ABSTRACT

As features on integrated circuits continue to grow smaller, they become more susceptible to damage from sequential planarization steps during fabrication. As planarization (known as chemical mechanical planarization, or simply CMP) is performed multiple times and on every stage of fabrication, potential damage from it represents a significant financial risk, motivating a more fundamental understanding of the material removal process. CMP typically consists of a stiff polymer pad being used to bring a chemically active colloidal suspension of nanoscale particles into contact and relative motion with the substrate to be polished. For narrow sets of conditions, CMP is typically seen to follow the Preston relation: material removal as a function of normal force and polishing distance. Modifications to the Preston equation have been made to relate wear volume to polishing friction force. A model has been developed for oxide CMP friction that segregated the frictional force generation into three regions: non-polishing bare-pad friction at the real pad-wafer contact sites, a pinned particle friction engaged in two-body particle abrasion at the real pad-wafer contact sites, and a swept region near the real contact engaging in three-body particle abrasion. The aim of this thesis is to advance the modified Preston relation with the novel model of friction to present a novel model that relates the wear volume to the work done by the two- and three-body particle abrasion, removing confounding non-polishing pad friction. The system studied was that of a fused silica wafer being polished with an alkaline silica particle suspension. A pin-on-disk tribometer was used for the frictional measurements and profilometry was used to determine the wear volumes. Independent wear factors were found for the pinned particles and the swept region of  $7.78\text{E-}11 \frac{\text{m}^3}{\text{N}\cdot\text{m}}$  and  $-9.94\text{E-}12 \frac{\text{m}^3}{\text{N}\cdot\text{m}}$  respectively. It is concluded that the polishing occurs at the pinned particle contact sites, and

that, while frictionally significant, the swept region does not meaningfully contribute to material removal.

## LIST OF FIGURES

Figure 1	Diagram of Lithography and etching, followed by deposition and polishing	1
Figure 2	Schematic of Chemical Mechanical Polishing set up	2
Figure 3	Diagram of asperity-wafer junction showing the pad-wafer contact, pinned particle region, and swept particle region.	4
Figure 4	Graph of the averaged coefficient of friction vs. time for a single experimental run.	14
Figure 5	Scatter plot of the Chemical Mechanical Polishing coefficient of friction vs. hydrated pad coefficient of friction	15
Table 1	Table of averaged values for Chemical Mechanical Polishing coefficient of friction and hydrated pad coefficient of friction	16
Table 2	Matrix of X and Y regions for each material pairing	16
Figure 6	Image of a leveled and zoomed profilometry trace used to calculate wear volume	17

Table 3 Permutation matrix of material comparisons for pinned and swept particle wear factors 18

**SYMBOLS USED IN THIS WORK**

V	Volume of substrate polished away	t	Duration of polishing in seconds
K	Classical Prestonian wear factor	D	Diameter of silica particles, 100nm
K <sub>x</sub>	Wear factor for pinned particle region	X	Area fraction of pinned particles
K <sub>y</sub>	Wear factor for swept region	Y	Area fraction of swept region
N	Total normal Load applied	H <sub>pad</sub>	General hardness of a pad
N <sub>tot</sub>	Total normal Load applied (same as N)	H <sub>pad1</sub>	Hardness of first pad in comparison
N <sub>pp</sub>	Normal load born by the pinned particles	H <sub>pad2</sub>	Hardness of the second pad in comparison
N <sub>pad</sub>	Normal load born by bare pad	PF	Hexagonal dens packing factor, 0.8
F <sub>CMP</sub>	Full friction of CMP	μ <sub>pp</sub>	Coefficient of friction of pinned particles
F <sub>pp</sub>	Friction provided by pinned particle	μ <sub>CMP1</sub>	Coefficient of friction for total polishing for pad 1
F <sub>R</sub>	Friction provided by Swept region	μ <sub>CMP2</sub>	Coefficient of friction for total polishing for pad 2
f <sub>pp</sub>	Normal force carried by a single pinned particle	μ <sub>pad1</sub>	Coefficient of friction for first bare pad
f <sub>par</sub>	Lateral removal force of a single particle	μ <sub>pad2</sub>	Coefficient of friction for second bare pad
s	Sliding speed of the contact region	A <sub>real</sub>	Area of real contact between pad and wafer
COF	Coefficient of Friction	A <sub>ap</sub>	Apparent area of contact between pad and wafer



B.A.R. Bearing area ratio

LDPE Low Density Polyethylene

CMP Chemical Mechanical Planarization

PTFE Polytetrafluoroethylene

## INTRODUCTION

Integrated circuit fabrication is vital to our information-driven modern world. The buildup of small electronic structures in an integrated circuit requires subsequent steps of lithography followed by deposition, and then the excess material is polished away to prepare for the next stage of lithography.<sup>1</sup> The critical factors of this polishing are removing material as well as achieving very precise planarization, as depicted below in Figure 1.

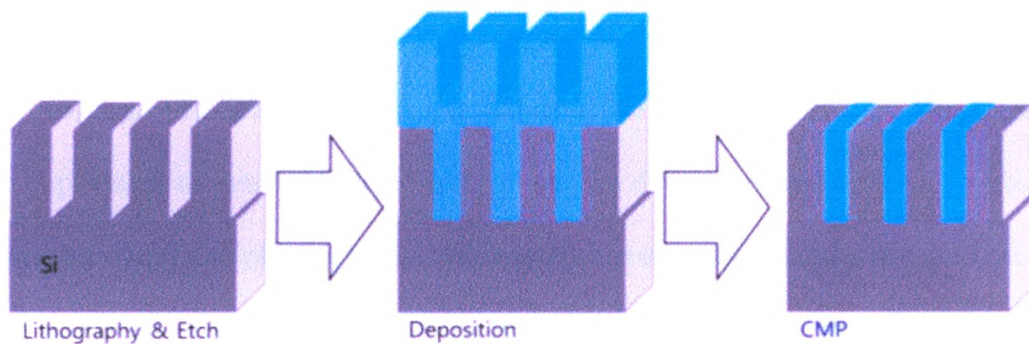


*Figure 1. Depiction of the Lithography and etching, followed by deposition, and finally polishing.<sup>2</sup>*

The chemical mechanical polishing of semiconductor wafers, hereafter referred to as CMP, is typically preformed using a soft hydrophilic fully-hydrated and conditioned polyurethane pad flooded with a chemically active colloidal suspension of silica or other abrasive particles that are often less than 100 nanometers in diameter.<sup>3</sup> The wafer containing a batch of integrated circuits is mounted on a carrier and pressed down onto the hydrated and conditioned pad in the presents of the slurry as shown in Figure 2. The pad and wafer are then slid against each other and it is this relative motion that causes polishing to occur.

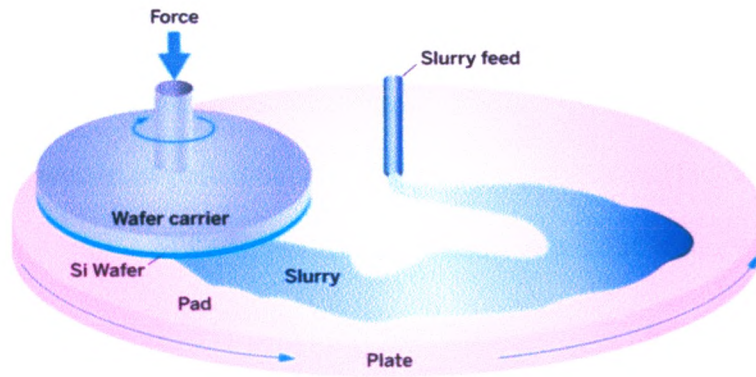


*Figure 2. Depiction of moving wafer against polishing pad in the presents of slurry*

The scale of electrical components continues to shrink, and integrated circuit designs continue to grow more complicated, requiring that the CMP process be repeated many more times. The implication of this is that near- and sub-surface defects become a more significant risk to the circuit structures, and planarizing the surface for late stage lithography becomes more crucial. The substantial financial risk that these processes represent are a motivation for a more explicit understanding of the material removal mechanism.<sup>4</sup>

Current models of oxide CMP typically assume that the alkaline nature of the slurry chemically modifies the wafer surface to soften it, and then suspended particles are trapped at asperity junction sites on the conditioned pad and engage in two-body abrasion.<sup>6</sup> For clarity, asperities are the microscopic peaks on a ‘flat’ pad surface that make physical contact with the wafer, and two-body abrasion is when the polishing grit is embedded in the pad, much like sandpaper. Furthermore, conditioning is the deliberate roughening of the pad to increase asperity density. It has been seen by Moon and others that the polishing could not have been done by the pad material itself, meaning that the polishing can be attributed to a combination of chemical and particle activity exclusively.<sup>7</sup> Most experimentation agrees that, within specified ranges, CMP abides a Preston-style relation, material removed is a linear proportion of the product of normal loading and sliding distance.<sup>3,8</sup>

$$V = K \cdot N \cdot s \cdot t \quad (1)$$

Where  $V$  is the volume removed during polishing,  $N$  is the normal force applied,  $s$  is the sliding speed,  $t$  is the duration of polishing, and  $K$  is the Prestonian wear factor. Typical values seen in industry are one micron of depth per area per minute when run with a 35kPa normal load at 0.5 m/s, resulting in a classical wear factor of  $K = 9.7 \times 10^{-13} \frac{m^3}{N \cdot m}$ . Moon et. al. showed a correlation between polishing friction and material removal per sliding distance, which advances the Preston relation from a virtual work term, normal force times distance, to an actual work term, friction force times distance

$$V = K \cdot F_{CMP} \cdot s \cdot t \quad (2)$$

where  $F_{CMP}$  is the measured friction during CMP and  $V$  is again the volume of material removed.<sup>7</sup>

It should be noted that an examination of polishing friction during CMP shows several counterintuitive trends. Basim was able to photograph slurry coated wafers showing a hexagonal dense-pack, indicating that the slurry will automatically cover a surface.<sup>9</sup> It has been seen by Taran et. al. that the coefficient of friction, here after called COF, of hydrated silica self-mated is much less than non-hydrated silica, ranging from 0.02-0.04 for hydrated silica.<sup>10</sup> Said another way, it would be expected that the polishing stage should report COF on the order of 0.03, however, Levert et al. measured typical CMP COF values on the order of .25-.35.<sup>11</sup> The conflict between the low friction of self-mated silica and the comparably high commonly-reported industrial COF of CMP is taken as indication that there is some portion of pad asperity making direct contact with the wafer, representing substantial friction in CMP that is not associated with material removal. Rimai et. al. was able to photograph the engulfment of nanoparticles on the surface of a pad suggesting that, in the short term, the nanoparticles on the pad could become

rarified at the asperity-wafer contact junction.<sup>12</sup> Asperity junction particle rarefication could explain why the friction does not fall to that of hydrated silica, but Levert et al. report not only a higher than expected friction, but that the polishing friction was higher than simply hydrated pad on hydrated silica.<sup>11</sup> One could relate this to adding a lubricant and seeing surface traction increase.

In an effort to resolve this counter intuitive result Levert et al. presented a friction model to separate the pad friction from the friction attributed to the slurry particles, referred to hereafter as “particle friction”.<sup>13</sup> The model considers the quasi-static asperity level mechanical interaction of the asperity-wafer junction. The model develops a force balance based in the normal and frictional forces for an asperity wafer junction consisting of three regions: pad-wafer contact, pinned particle-wafer contact, and a novel region surrounding the asperity where particles are indirectly agitated by the asperity termed “the swept region.”

$$\text{Frictional Force} = \mu_{pp} \cdot N_{pp} + \mu_{pad} \cdot N_{pad} + F_R \quad (3)$$

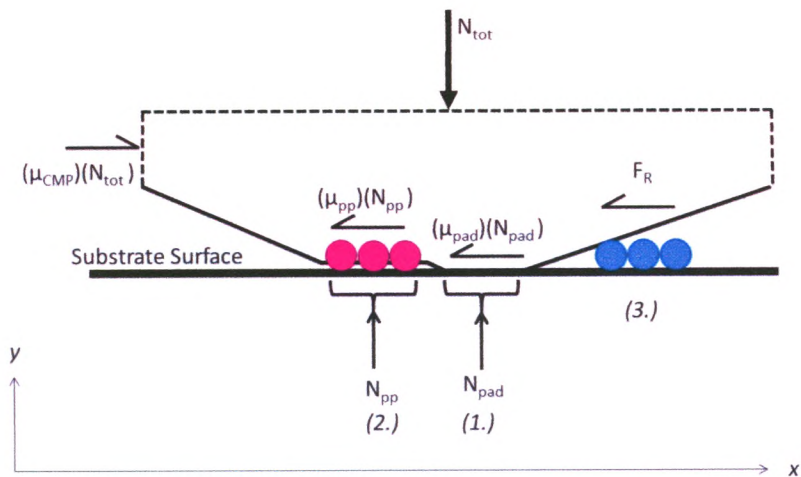


Figure 3. Normal and Lateral forces applied at the asperity-wafer junction. Image taken with permission from Levert et. al.<sup>9</sup>

The normal loads on the pad and pinned particles,  $N_{pad}$  and  $N_{pp}$  respectively, are taken to be the pad's material hardness times the real contact of each area and must sum to the total normal load,  $N_{tot}$ . The total friction force of polishing is taken as a COF,  $\mu_{CMP}$ , times the normal load. The balancing lateral forces are taken to be the contact normal loads scaled by their respective coefficients,  $\mu_{PP}$  and  $\mu_{pad}$ , plus a force per unit area value for the swept region,  $F_R$ . The force balance is used to generate a system of two equations relating polishing friction to pad hardness which return the relative areas of each region when solved simultaneously.

$$0 = X(H_{Pad1})[\mu_{pad1} - \mu_{pp}] + Y[F_R] + (H_{Pad1})[\mu_{CMP1} - \mu_{pad1}] \quad (4)$$

$$0 = X(H_{Pad2})[\mu_{pad2} - \mu_{pp}] + Y[F_R] + (H_{Pad2})[\mu_{CMP2} - \mu_{pad2}] \quad (5)$$

Where X is the area of the asperity covered in particles relative to the total real contact, Y is the area of the swept region relative to the real contact, and  $F_R$  is the friction provided by the swept region per unit area. Levert's work suggests that the pad junction area with significant particle contact is only 18% of junction area, and the swept area, pushed in front of asperity junctions, is about 3800% of the junction area. This work was based on the oxide CMP process because it is a well-explored system and any results from this oxide system may be more easily extended to other CMP processes. In this paper, Levert's friction work is used to extended Moon's modified Preston equation by comparing the wear rates of the silica substrate to the friction attributed to particle friction, resulting in two Preston-style wear coefficients: a swept particle wear factor and a pinned particle wear factor.

## MODEL

This paper assumes a friction model presented by Levert et. al. in Tribology Transactions in 2019.<sup>11</sup> The model considers the asperity level mechanics at the asperity-wafer junction sites, specifically identifying three distinct regions: bare pad, pinned particles, and swept particle regions. The bare pad region is taken to be the portion of the real pad contact that is free of slurry nanoparticles where friction would come solely from pad-substrate adhesion and is assumed to do no polishing. The bare pad region could be a result of either incomplete coverage by the nanoparticles or by particle rarefaction due to engulfment by the pad. The pinned particle region is taken to be the portion of the real pad contact where the asperity has pinned a slurry nanoparticle between the substrate and itself and is considered the classic source of polishing. These particles bear the full pressure equivalence of the pad hardness. The third, and novel, region is the swept particle region, which is taken to be an area extending in front and to the sides of the asperity-wafer junction. It is the belief of the author that this region may be responsible for a statistically significant portion of the polishing friction.

By varying the pad material between runs, the model returns the fraction of the real contact area covered in pinned particles,  $X$ , and the area of the swept region as a multiple of the real contact area,  $Y$ .

The purpose of this investigation is to extend the work done by Levert et. al. by creating an enhanced Prestonian relation capable of parsing the polishing performed by the pinned particles from that of the swept region without the confounding friction of the pad.<sup>11</sup> To begin, we start with Moon's adaptation of Preston's relation, Equation 2

$$V = K \cdot F_{CMP} \cdot s \cdot t \quad (2)$$

where  $F_f$  is the force of friction measured during polishing and modify by replacing it with the force of friction provided solely by the slurry, as modeled by Levert<sup>9</sup> et. al.

$$V = K \cdot [F_{pp} + F_R] \cdot s \cdot t \quad (6)$$

where  $F_{pp}$  is the frictional force from pinned particles and  $F_R$  is the force provided by the swept particles. To calculate the friction force contributed by the pinned particles, one must consider the force per particle, the number of particles, and the COF of hydrated fused silica self-mated. The friction force per pinned particle can be approximated as the cross-sectional area of a single particle times the strength of the material and the self-mated silica COF

$$f_{pp} = \mu_{pp} H_{pad} \cdot \frac{\pi D^2}{4} \quad (7)$$

Where  $f_{pp}$  is the friction force per pinned particle,  $\mu_{pp}$  is the self-mated COF of modified silica as measured by Choi,  $H_{pad}$  is the hardness of a given pad, and  $D$  is the diameter of a single particle.<sup>4</sup> The number of particles involved in supporting the pad can be estimated using the fraction of asperity coverage,  $X$ , determined from the friction data by dividing real-and-covered contact area by the area per particle

$$Particle\ count = X \cdot \frac{N}{H_{pad}} \cdot \frac{4}{\pi D^2} \quad (8)$$

It should be noted that the asperity deformation is taken to be fully plastic at this scale, implying that the ratio of normal load to pad hardness is considered equivalent to the real contact area. Multiplying (7) and (8) returns the total normal load carried by the pinned particles. Conveniently, this causes both pad hardness and particle size to cancel out. The total frictional force contributed by the pinned particles can be estimated by multiplying the full pinned particle



normal load by the literature value of the COF for self-mated hydrated silica,  $\mu_{pp}$ . The resulting expression for the total friction contributed by the pinned particles is

$$F_{pp} = \mu_{pp} \cdot X \cdot N \quad (9)$$

To quantify the frictional force contributed by the swept region, one must consider the force per particle in conjunction with the number of particles. The number of particles can be estimated by dividing the total area of the swept region by the size per particle. The total area is given by the real contact, normal load [N] divided by pad hardness [ $H_{pad}$ ], times the swept region fraction [Y]. Finally, one can multiply this value by the lateral removal force per particle  $f_{par}$

$$F_R = \frac{Y \cdot N}{H_{pad}} \cdot \left[ \frac{\pi D^2}{4} \right]^{-1} \cdot PF \cdot f_{par} \quad (10)$$

where PF is the dense hexagonal packing factor of 0.8, as was seen by Basim et. al. The value  $f_{par}$  is taken to be 0.5 nN, as measured by Choi.<sup>7,12</sup> By substituting these two terms into our enhanced Prestonian relation, equation we arrive at

$$V = K \cdot \left[ \frac{Y \cdot N}{H_{pad}} \cdot \frac{4 \cdot PF}{\pi D^2} \cdot f_{par} + X \cdot \mu_{pp} \cdot N \right] \cdot s \cdot t \quad (11)$$

Finally, we can pull the normal load out of both terms and assign specialized K values,  $K_{pp}$  and  $K_s$  respectively, resulting in the final iteration of the enhanced Prestonian relation

$$V = \left[ K_y \left( \frac{Y}{H_{pad}} \cdot \frac{4 \cdot PF}{\pi D^2} \cdot f_{par} \right) + K_x \cdot X \cdot \mu_{pp} \right] \cdot N \cdot s \cdot t \quad (12)$$

The formulation preserves the assumption that the X and Y regions are largely pad-independent values implying the only independent variable in the system is the pad hardness with only two unknowns:  $K_y$  and  $K_x$ . Therefore, this can be rearranged to have the measured value equated to a linear combination of the two unknowns

$$\frac{V}{s \cdot t \cdot N} = K_y \left( \frac{Y}{H_{pad}} \cdot \frac{4 \cdot PF}{\pi D^2} \cdot f_{par} \right) + K_x \cdot X \cdot \mu_{pp} \quad (13)$$

By varying the pad hardness and measuring the resulting polishing, this equation can be made into a system of two equations and converted to matrix form

$$\begin{bmatrix} \frac{V_1}{s \cdot t \cdot N} \\ \frac{V_2}{s \cdot t \cdot N} \end{bmatrix} = \begin{bmatrix} \frac{Y}{H_{pad1}} \cdot \frac{4 \cdot PF}{\pi D^2} \cdot f_{par} & X \cdot \mu_{pp} \\ \frac{Y}{H_{pad2}} \cdot \frac{4 \cdot PF}{\pi D^2} \cdot f_{par} & X \cdot \mu_{pp} \end{bmatrix} \begin{bmatrix} K_y \\ K_x \end{bmatrix} \quad (14)$$

This matrix can then be inverted and multiplied through to generate an equation for each unknown

$$K_y = \frac{X \cdot \mu_{pp} \cdot \frac{V_1}{s \cdot t \cdot N} - X \cdot \mu_{pp} \cdot \frac{V_2}{s \cdot t \cdot N}}{\frac{Y}{H_{pad1}} \cdot \frac{4 \cdot PF}{\pi D^2} \cdot f_{par} \cdot X \cdot \mu_{pp} - \frac{Y}{H_{pad2}} \cdot \frac{4 \cdot PF}{\pi D^2} \cdot f_{par} \cdot X \cdot \mu_{pp}} \quad (15)$$

$$K_x = \frac{\frac{Y}{H_{pad1}} \cdot \frac{4 \cdot PF}{\pi D^2} \cdot f_{par} \cdot \frac{V_2}{s \cdot t \cdot N} - \frac{Y}{H_{pad2}} \cdot \frac{4 \cdot PF}{\pi D^2} \cdot f_{par} \cdot \frac{V_1}{s \cdot t \cdot N}}{\frac{Y}{H_{pad1}} \cdot \frac{4 \cdot PF}{\pi D^2} \cdot f_{par} \cdot X \cdot \mu_{pp} - \frac{Y}{H_{pad2}} \cdot \frac{4 \cdot PF}{\pi D^2} \cdot f_{par} \cdot X \cdot \mu_{pp}} \quad (16)$$

These equations have as experimental inputs only volumes of wear for each material and the X and Y area fractions, which are considered, from the work by Levert, to be approximately pad-independent over a narrow range of hardnesses.

## TEST PROCEDURE

The test procedure consists of 5 stages: pad material sample preparation, fused silica wafer cleaning, slurry preparation, friction trace testing, and finally profilometry.

The pad material samples selected were IC1000 polyurethane industrial CMP pad, polytetrafluoroethylene [PTFE], and low-density polyethylene [LDPE]. These materials were selected because they have similar hardnesses but vary in their coefficient of friction [COF] when mated against hydrated fused silica.

Sample preparation involved cleaning the sample with isopropyl alcohol and distilled water. The pad was then allowed to dry for 24 hours to minimize the presence of adhered alcohol. Once fully dry, the pad was soaked in distilled water for 72 hours to ensure that the sample was stably hydrated.<sup>15</sup>

The fused silica wafers were cleaned using the first stage of the Radio Corporation of America's semiconductor cleaning protocol. The first stage of the cleaning, known as SC1, was intended to remove organic contaminants from the silica wafer. This consisted of soaking the wafers for 30 minutes in a hot bath of 30% ammonium hydroxide, 15% hydrogen peroxide, and distilled water mixed in a 1:2:4 ratio before rinsing them with distilled water. The wafers were then allowed to dry for 12 hours to ensure that the wafer surface was not in a chemically-modified state at the beginning of the test. Several months were lost to establishing the cleaning procedure, which ultimately out of necessity included pre-washing all glassware and samples with alcohol before rinsing with the SC1 solution prior to cleaning. It was then discovered that the gloves being used to clean the glassware were contributing a surfactant and had to be replaced with specialty gloves that do not use a mold-release agent.

The polishing slurry was prepared suspending 100-nanometer diameter fused silica spheres in ammonia water diluted to a pH of 11.5 in a 5% by weight concentration. The pH of 11.5 was used because it minimized the chance for aggregation of the silica particles.<sup>16</sup> The concentration of 5% by weight was selected to align with common oxide-polishing procedures.<sup>17</sup> This differs from work done by Levert because it was shown that the friction sensitivity to concentration decreases beyond 5 % by weight.<sup>18</sup> In an effort to ensure consistent slurry behavior over several tests we pushed the concentration up to a region where small fluctuations would be less impactful on results. Once the silica spheres were added to the diluted ammonium hydroxide, they were placed in an ultrasonic cleaner for 4 hours to ensure colloidal suspension of the spheres in solution. This represented the final iteration of the polishing slurry, as earlier versions did not have the stability over time necessary to maintain consistency across experimental runs. A lack of additives in the solution made particles tend to agglomerate quickly and fall out of colloidal suspension. By increasing the percent weight from one to five, we saw a much more consistent bulk slurry solution.

The friction measurement was taken on a pin-on-disk tribometer with independent normal force and lateral force load cells. The normal load cell captured the applied force, while the lateral load cell captured the resulting frictional force. The stylus pin had a radius of curvature of 5 mm and was placed so the drawn track had a radius of 5 mm. The normal load applied was 50 grams to generate an average contact stress of 7.6 MPa. The disk mount for the wafers was rotated such that the contact point was passing the stylus at 6.8 mm per second. These speeds were used to avoid any hydrodynamic lubrication effects and were seen by Levert et. al. to maintain representative coefficients of friction.<sup>11</sup>

Each trial started with mounting the wafer and pad samples in clean conditions. The position of the wafer in relation to the turntable was measured from three positions for triangulation during profilometry. The pad sample was then mounted on the stylus and suspended over the turntable. Data collection was started to record the zero point of the sensors before dilute ammonium hydroxide of pH 11.5 was applied to the wafer and the pad was lowered into contact. The 50-gram load was added and the table's rotation was initiated. After the behavior had stabilized (60-90 seconds), the sample was run for another 200 seconds to establish the baseline pad friction coefficient. The polishing slurry was then added; sufficient slurry was used to flush the full surface of the wafer to ensure that the concentration at the polishing site was representative of the overall slurry properties. Slurry was added in 1.5 ml increments every 100 seconds to ensure pH stability and slurry concentration throughout the duration of the polishing. Polishing was performed for 1500 seconds to encourage a measurable track depth. At the end of the run, the beam supporting the stylus was lightly touched to time-stamp both the normal and lateral load cells. The time stamp enabled chronological calibration of both the normal and lateral load cells.

For profilometry, the track position was estimated by the triangulation points on a paper mat on which the wafer was then placed. The paper mat was lightly wetted to secure the wafer in place. A Taylor Hobson Surtronic S-100 series contact stylus profilometer was used. It employed a skidded diamond stylus tip with a five micron radius and 5 nanometer resolution. A typical trace was 12.5 mm long. The data was visualized in TalyProfile Lite 6.2. Eight radial traces were recorded and all indicators were plotted on a radial chart. For indicators that formed a circular track the trace was leveled and zoomed in so that the area of the trough could be manually

counted. These areas were averaged and multiplied by the circumference of the track (0.0314m) to estimate the wear volume.

The friction data was processed with the friction model presented by Levert et. al. to establish a value for the magnitude of the swept region in front of the asperity and the percent-coverage of the asperity contact area.<sup>11</sup> These values were then used in the novel modified Preston equation presented in this paper, in conjunction with the wear volume data, to determine independent wear factors for the swept-particle action and the pinned-particle action.

## RESULTS

The acquired data for the normal and lateral force traces were temporally aligned to within one tenth of a second. At each time step, the lateral force was divided by the normal force to calculate an instantaneous COF, then any negative values or values in excess of one were discarded. While values in excess of one are not theoretically impossible, no such values are ever seen during polishing and are taken categorically to be artifacts of experimental setup and handling. A forward-running average of thirty seconds, or three hundred points, was taken to smooth out the friction trace, as it represented several full rotations of the sample and was free of local physical features. A typical plot of the running friction is depicted in figure 2 with blue.

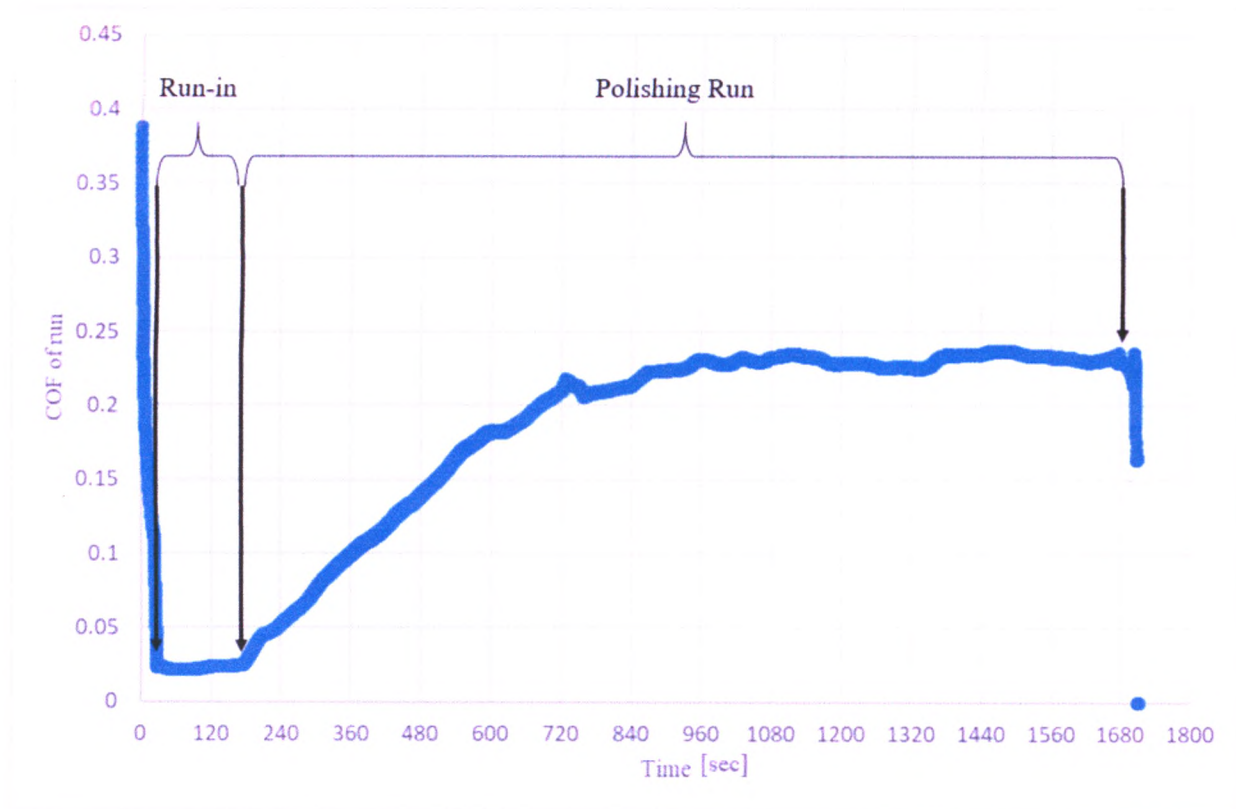


Figure 4. Pad COF is the baseline COF for the bare pad in an ammonia solution. Polishing run refers to after the addition of slurry

It can be clearly seen that COF increases from the baseline pad friction at the addition of slurry. To rule out fluid behaviors as a source of the force, sensitivity to hydrodynamic forces was evaluated. Asperity features were assumed to be spaced an average distance of ten microns apart and to be one micron tall, based on measurements presented by Choi.<sup>14</sup> Contact path size was taken from observations made during polishing trials, which were in agreement with Hertzian sphere on flat predictions. It was found that the dynamic viscosity of the slurry would need to be approximately five orders of magnitude greater than that of the ammonia solution in order to have this increase in force be attributable to viscous effects, further suggesting that polishing action must be responsible for the increased force during polishing.

The COF attributed to the pad was pulled from thirty-one seconds before the addition of the slurry to ensure that it was not artificially elevated by the averaging process. The COF values from the point of slurry addition until the end of the run were averaged to determine a COF of CMP. Figure 3 shows COF of CPM plotted against pad COF for individual runs grouped by material.

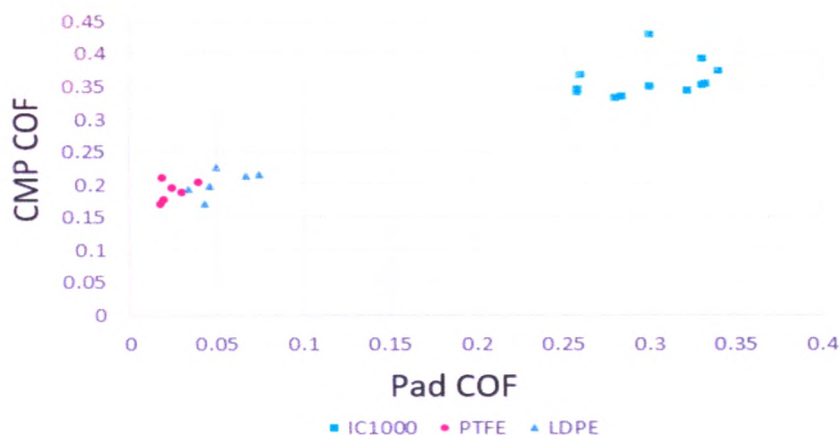


Figure 5. plot of the CMP COF as a function of Pad COF. Squares are ICI1000, Triangles are LDPE, and Circles are PTFE.



Typical values for the pad and CPM COF can be seen in table 1.

Table 1. Pad and CMP coefficients of friction

	IC1000	LDPE	PTFE
Pad COF	0.300	0.0525	0.0252
CMP COF	0.359	0.202	0.186

Pairs of materials were processed with the Levert model of friction to calculate the X and Y regions. The resulting X and Y regions from each pairing are displayed in Table 2.

Table 2. Fractional X and Y regions for each material pairing as compared to real asperity contact region

Pad 2	Pad1 -->	IC100	LDPE	PTFE
IC1000	X		0.684	0.647
	Y		93.1	89.3
LDPE	X	0.684		0.429
	Y	93.1		91.2
PTFE	X	0.647	0.429	
	Y	89.3	91.2	

The values collected during this experiment suggested an X region, the fraction of asperity covered in particles, to be 59% of the real contact area, while the data suggested a Y region, the swept particle field, to be on the order of 9100% of the real contact area.

Polished trough profiles were measured with a Surtronic S-100 series surface profilometers with a 5-nanometer radius stylus tip. Once radial traces were taken and signals selected as representative of a trough, they were processed in the TalyProfile Lite free downloadable software associated with the Surtronic. Traces were leveled and then enlarged at the sections of interest, the backgrounds removed, and the raw trace is measured against a scaled grid in the program's user interface. Figure 3 is an example profilometry trace. A typical window was 55 grid squares high with a range of one micron and 85 grid squares wide

representing half a millimeter. Cross sections were typically on the order of 500 grid squares in area, or  $5 \cdot 10^{-11} \text{ m}^2$ . The cross sections for a given polishing trough were averaged and multiplied by the track circumference to approximate the polishing volume, typically on the order of  $5 \cdot 10^{-13} \text{ m}^3$ .

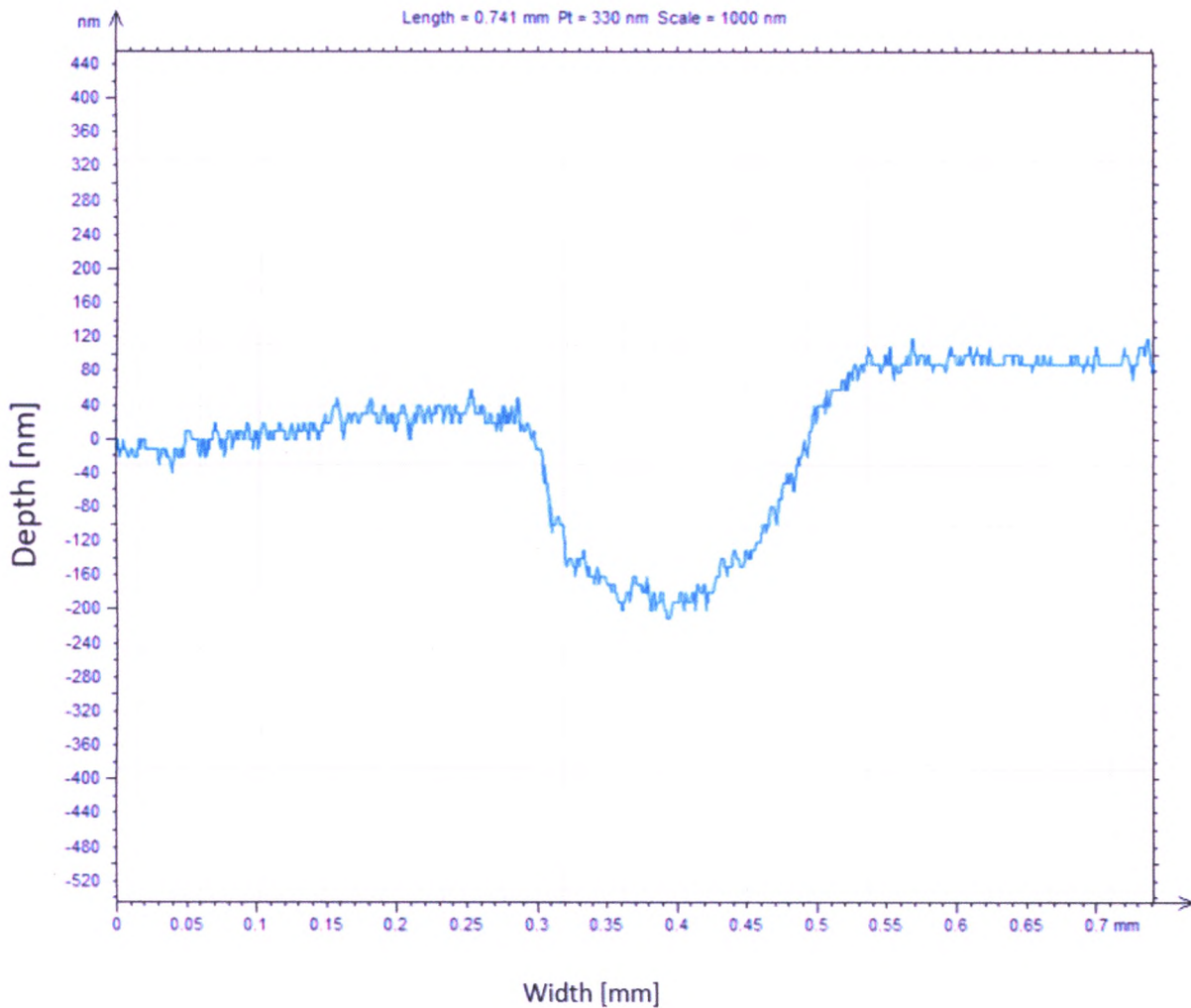


*Figure 6. Typical Profilometry trace. Window is 0.741 mm wide and 330 nm tall*

It should be noted that only a limited number of usable polishing runs were successful at forming a measurable track and that the sample size for IC1000, LDPE, and PTFE are one, two, and four respectively. This was due in part to the extreme difficulty in collecting data, each point representing a six-hour investment made over 5-7 days with a high interference rate.

At this point, the wear volumes were used to calculate a classical Prestonian wear factor as a check for reasonability. It was found that these pads showed an average classical wear factor of  $2.67\text{E-}13 \frac{\text{m}^3}{\text{N}\cdot\text{m}}$  which was about a quarter of the representative value given in the introduction. For a tribological system this is taken as strong agreement, suggesting that the wear values found in the experiment are representative of actual polishing rates.

The X and Y values from the friction measurements were taken together with pairs of wear volumes found in the profilometry and interpreted through equations (15) and (16). The table below details the results of these combinations.

*Table 3. Wear factors  $K_x$  and  $K_y$  as calculated by each material pair*

2	1-->	IC1000	PTFE	LDPE
IC1000	$K_x$		2.22E-11	3.44E-13
	$K_y$		-1.11E-12	1.10E-12
PTFE	$K_x$	2.22E-11		1.31E-10
	$K_y$	-1.11E-12		-1.88E-11
LDPE	$K_x$	3.44E-13	1.31E-10	
	$K_y$	1.108E-12	-1.88E-11	

An average value for  $K_x$  was taken to be  $7.78\text{E-}11 \frac{\text{m}^3}{\text{N}\cdot\text{m}}$  and the averaged value for  $K_y$  was taken to be  $-9.94\text{E-}12 \frac{\text{m}^3}{\text{N}\cdot\text{m}}$ . The pairs averaged were PTFE vs. IC1000 and PTFE vs. LDPE. LDPE vs. IC1000 was not averaged in because data was too scarce for these to give a reasonable confidence in the comparison to one another.

## DISCUSSION

### Overview

Moon proposed a modified Preston equation where the force term was switched from normal force applied to friction force measured, Equation (2), making the right side of the Preston equation more closely represent a work term.

Levert put forth a model of friction in CMP that aimed to separate the non-polishing pad friction from the slurry activity. In this investigation the work of Moon and Levert are combined to refine equation (2) into a relation between volume of polishing and the work done solely by the polishing mechanism; slurry activity. By virtue of the Levert model describing the spatial relationship of friction to the asperity contact area, relating the material removal to the friction contributors helps to shed light on the physical location of polishing with respect to the asperity.

### Friction

A comparison of the X and Y regions found in this experiment (59% and 9100% of the real contact area respectively) finds them to be in good agreement with previous work done by Levert et. al., who reported X and Y regions of 18% and 3800% of the real contact area respectively. For a tribological system, these are considered to agree strongly in their own right, but the comparison grows more robust when the differences in polishing time and slurry concentration are considered. In the current experiment, the polishing times are approximately three and a half times longer than in the work done by Levert, which could have led to significantly more pad self-conditioning than in previous work, elevating the reported friction values. Furthermore, the slurry used in this experiment was five times greater in particle concentration, which could conceivably extend the special range at which the asperity holds

sway. In light of these factors, the agreement between these values is taken to suggest that the current experiment has successfully reproduced the previous work on friction.

It is worth asking, at this point, whether these values could still hold physical meaning. Hutchings suggests that by considering the pad hardness and the force applied, one can estimate the real contact area assuming plastic asperity deformation by the relation: <sup>17</sup>

$$A_{real} = \frac{N}{H_{pad}} \quad (17)$$

Given this, one can consider the bearing area ratio, or B.A.R., by taking the ratio of the real contact area to the apparent contact area. For a pad like IC1000 with a hardness of 32 MPa and a loading of 50 grams, this results in an estimated real contact area of  $1.5 \cdot 10^{-8} \text{ m}^2$ . Measured apparent contact areas ranged from  $1.96 \cdot 10^{-7} \text{ m}^2$  to  $1.77 \cdot 10^{-6} \text{ m}^2$ . These values provide a B.A.R. in the range of 7.6%-0.8%, with the expectation that the most reputable value is towards the lower end of this range. Comparing these real contacts with the swept region (being 40 to 90 times larger) shows that the Y region is on the order of the apparent contact zone. While this represents a rather extreme case, it is taken to be plausible, as in industry one would typically see lower normal loads and shorter polishing times.

## **Wear**

The wear factors calculated from the profilometry suggest that the pinned particle wear factor,  $K_x$ , is at least an order of magnitude greater than the swept region wear factor,  $K_y$ , and possibly of the opposite sign. In fact, the model suggests that if two pads were to have the same material removal rate then  $K_Y$  would go to zero. We suggest from this that the swept region does not contribute to material removal rate in a meaningful way, and that the polishing does occur at the asperity-wafer junction. This trend is in support of the classical interpretation of CMP, such

as proposed by Lin et. al. <sup>4</sup> To the knowledge of the author, this has often been assumed to be true, but has, to date, gone unsubstantiated.

Particles in the Y region are thought to be jostled by each other and by viscous forces at a distance from the asperity. It may be that these particles are ploughing the hydrated silica layer or adhering and subsequently being swept off, changing its morphology without significantly affecting material removal rate. Furthermore, if the negative wear factor is real, there may be local deposition of silica from particle or slurry solution onto the surface. In either case, while the Y region does not contribute to material removal rate, it certainly contributes to friction suggesting it likely still plays a role in surface finish and morphology, such as shallow trench isolation, or edge rounding on small features in late stage integrated circuit fabrication.

The accuracy of these wear factor values,  $K_Y$  and  $K_X$ , is low due to the extremely small sample size for wear values. There was a total of five usable points for PTFE, two for LDPE, and only one for IC1000. As the model is an empirical one, and therefore does not claim to fully capture the mechanics, it suggests that a sensitivity analysis of the novel polishing relation would not be fruitful. Furthermore, the number of successful comparisons is too few to make a meaningful statistical confidence analysis, implying that the results from this investigation are suggestive of possible trends, but are not definitive.

The lack of usable points is due in large part to the challenges inherent in the experiment. Each data point represents many hours of work over several days and is subject to a high failure rate. Most significantly, there was a common issue where a total lack of polishing was observed across many pad materials, particularly with the IC1000. It is suspected that the slurry chemistry is the driving factor behind the lack of polishing, as the physical parameters that are controllable were extensively varied without successfully making polishing regular. The slurry used in this

experiment is the simplest possible slurry that can be prepared: silica spheres suspended in an ammonia solution with no other surfactants. The simplicity of the slurry comes from the work done by Levert et. al., and was deliberate to help uncouple the physical and chemical parameters in polishing.<sup>9</sup> It appears that this is an oversimplification that has ultimately reduced the repeatability of the experiment in a significant way.

### **Future work**

Future iterations of this experiment could benefit from the use of industrial slurry and a specially prepared solution that is comprised of the base and additives in the slurry without the suspended polishing particles. By reincorporating the other surfactants, the experiment may behave more closely to industrial polishing and return more repeatable material removal. In addition to using a new slurry to help improve repeatability, the implementation of pad preconditioning would help to bring this investigation more into line with industrial practices. Pad conditioning had been left out of this work, as no effective repeatable roughening protocol was able to be found for several of our materials.

Another consideration that should be captured by future work is related to the determination of the X and Y regions: it is assumed that particle engulfment is similar across pad materials, implying that the X and Y regions are identical across each material, which is likely not true. The assumption was made primarily to make the system of equations solvable, and in an effort to support its reasonability, all pad hardnesses were kept within a factor, normalizing real contact area. By normalizing the real contact area and assuming engulfment consistent across materials, one is functionally asserting that the pinned particle region has the same gross extent between materials, something not yet shown to be true. It may be possible to reconstruct the force balance in the Levert friction model so that the normal force is varied between runs, rather

than varying pad material, as a way of backing out the X and Y regions. Doing this would allow the experiment to determine a material-specific X and Y region which would make the use of these values more internally consistent.



## CONCLUSION

A modified version of Preston's equation presented by Moon was combined with Levert's model of slurry friction to create a novel relationship between material removed during polishing and the work performed by the slurry that directly contributes to material removal. Of the three sources of friction considered, pad-wafer contact, pinned-particle friction, and swept particle friction, only two sources of work were considered to contribute to polishing. As modeled by Levert these were the pinned particles at asperity-wafer junctions and a swept region of particles adhered to the wafer outside of the asperity contact site that are still being moved by local motion. Levert had suggested these two regions as an explanation of the counterintuitive increase in COF with the addition of polishing slurry. Friction results from this experiment are in agreement with Levert's findings – strengthening the suggestion that a very significant portion of the pad asperity junction has bare-pad-to-substrate interaction. The findings suggest active particle areas of  $X = 50\%$  for pinned particles and  $Y = 9100\%$  for swept particles with respect to the real contact area. Wear factors for both sources of anticipated material removal were calculated from the experimental data. The averaged wear factor for the pinned particles,  $K_X$ , was found to be  $7.78E-11 \frac{m^3}{N \cdot m}$ , and the averaged wear factor for the swept region,  $K_Y$ , was found to be  $-9.94E-12 \frac{m^3}{N \cdot m}$ . The pinned particle value was found to be around two orders of magnitude greater than the classical wear factor, which is in alignment with Moon's findings. The disparity between the pinned particle wear factor and the swept region wear factor suggests that the polishing in CMP does, in fact, take place at the asperity-wafer junction and is performed by the pinned particles there. These findings are in support of the traditional view of material removal.

A possible interpretation of the negative value for the swept region could be a deposition process of silica out of the slurry on to the surface. However, the low confidence in the precision of this value makes it arguably indistinguishable from zero. While it appears that the swept region does not significantly contribute to the polishing, it is not clear whether its role in polishing can be ignored. It may still play a role in surface finish, such as single trench isolation or edge rounding of small features. In light of this, there may be a way to help tune the sensitivity to material removal and edge rounding through controlling the interplay of the pinned and swept regions by adjusting the pad material micro-hardness.

## WORKS CITED

1. Steigerwald, J. M., Murarka, S. P., & Gutmann, R. J. (2004). *Chemical mechanical planarization of microelectronic materials*. Weinheim: Wiley-VCH.
2. Kim, H. J. (2018). Abrasive for chemical mechanical polishing. In *Abrasive Technology - Characteristics and Applications*. (183-201) doi: 10.5772/intechopen.75408
3. Lee, H., Jeong, H., & Dornfeld, D. (2013). Semi-empirical material removal rate distribution model for SiO<sub>2</sub> chemical mechanical polishing (CMP) processes. *Precision Engineering*, 37(2), 483-490. doi:10.1016/j.precisioneng.2012.12.006
4. Choi, J. H., & Korach, C. S. (2009). Nanoscale defect generation in CMP of low-k/copper interconnect patterns. *Journal of The Electrochemical Society*, 156(12). doi:10.1149/1.3243852
5. Tullo, A. H. (n.d.). Electronic Chemical Makers Help Keep Gordon Moore's Prediction Alive. Retrieved from <https://cen.acs.org/articles/93/i27/Electronic-Chemical-Makers-Help-Keep.html>.
6. Lin, Z., Wang, R., & Ma, S. (2018). Theoretical model and experimental analysis of chemical mechanical polishing with the effect of slurry for abrasive removal depth and surface morphology of silicon wafer. *Tribology International*, 117, 119-130. doi:10.1016/j.triboint.2017.08.021
7. Moon, Y. (1999). Mechanical aspects of the material removal mechanism in chemical mechanical polishing (CMP), Ph.D. dissertation, University of California, Berkeley.
8. Preston, F. W. (1926). The nature of the polishing operation. *Transactions of the Optical Society*, 27(3), 181-190. doi:10.1088/1475-4878/27/3/302

9. Basim, G., Vakarelski, I. U., & Moudgil, B. M. (2003). Role of interaction forces in controlling the stability and polishing performance of CMP slurries. *Journal of Colloid and Interface Science*, 263(2), 506–515. doi: 10.1016/s0021-9797(03)00201-7
10. Taran, E., Donose, B. C., Vakarelski, I. U., & Higashitani, K. (2006). PH dependence of friction forces between silica surfaces in solutions. *Journal of Colloid and Interface Science*, 297(1), 199-203. doi:10.1016/j.jcis.2005.10.038
11. Levert, J. A., Korach, C. S., Mooney, B., & Lynam, F. (2019). Model of particle contact area for friction in oxide chemical mechanical polishing. *ECS Journal of Solid State Science and Technology*, 8(9).
12. Rimai, D., Quesnel, D., & Busnaina, A. (2000). The adhesion of dry particles in the nanometer to micrometer-size range. *Colloids and Surfaces A: Physicochemical and Engineering Aspects*, 165(1-3), 3-10. doi:10.1016/s0927-7757(99)00439-2
13. Levert, J. A., Mess, F. M., Salant, R. F., Danyluk, S., & Baker, A. R. (2008). Mechanisms of chemical-mechanical polishing of SiO<sub>2</sub> dielectric on integrated circuits. *Tribology Transactions*, 41(4), 593-599. doi:10.1080/10402009808983787
14. Choi, J. H. (2009). Measurements of friction and wear in chemical mechanical polishing using single particle analog probes, Ph.D. dissertation, Stony Brook University.
15. Ng, S. H., Hight, R., Zhou, C., Yoon, I., & Danyluk, S. (2003). Pad soaking effect on interfacial fluid pressure measurements during CMP. *Journal of Tribology*, 125(3), 582–586. doi: 10.1115/1.1538632

16. Khanna, A. J., Gupta, S., Kumar, P., Chang, F.-C., & Singh, R. K. (2018). Study of agglomeration behavior of chemical mechanical polishing slurry under controlled shear environments. *ECS Journal of Solid State Science and Technology*, 7(5). doi: 10.1149/2.0091805jss
17. Seo, Y.-J. (2005). Oxide-chemical mechanical polishing characteristics using silica slurry retreated by mixing of original and used slurry. *Microelectronic Engineering*, 77(3-4), 263–269. doi: 10.1016/j.mee.2004.11.015
18. Levert, J. A., & Korach, C. S. (2009). CMP friction as a function of slurry silica nanoparticle concentration and diameter. *Tribology Transactions*, 52(2), 256-261. doi:10.1080/10402000802593130
19. Hutchings, I. M. (2003). *Tribology: friction and wear of engineering materials*. Oxford: ButterWorth-Heinemann.